








Original Research

Combined Use of Intranasal Methylprednisolone and Allopregnanolone: Revisiting Anti-inflammatory and Remyelinating Treatment in a Murine Model of Multiple Sclerosis

Iván Nicolás Pérez-Osorio¹, José Alejandro Espinosa-Cerón¹,
Camila Álvarez-Gutiérrez^{1,†}, Rodrigo Gonzalez-Flores^{1,†}, Hugo Besedovsky²,
Gladis Frago^{1,*}, Mónica A. Torres-Ramos^{3,4,*}, Edda Sciutto^{1,*}

¹Department of Immunology, Institute of Biomedical Research Universidad Nacional Autónoma de México, UNAM, 04510 Mexico City, Mexico

²Research Group Immunophysiology, Division of Neurophysiology, Institute of Physiology and Pathophysiology, Philipps Universität, 35037 Marburg, Germany

³Research Directorate, National Institute of Neurology and Neurosurgery Manuel Velasco Suárez, Tlalpan, 14269 Mexico City, Mexico

⁴Laboratory 4 Translational Sciences, Center for Research on Aging, CINVESTAV South Headquarters, 14330, Mexico City, Mexico

*Correspondence: gladis@unam.mx (Gladis Frago); monica.torres@innn.edu.mx (Mónica A. Torres-Ramos); edda@unam.mx (Edda Sciutto)

†These authors contributed equally.

Academic Editor: Thomas Heinbockel

Submitted: 20 August 2024 Revised: 30 October 2024 Accepted: 6 November 2024 Published: 18 December 2024

Abstract

Background: Multiple sclerosis (MS) is a demyelinating, neuroinflammatory, progressive disease that severely affects human health of young adults. Neuroinflammation (NI) and demyelination, as well as their interactions, are key therapeutic targets to halt or slow disease progression. Potent steroidal anti-inflammatory drugs such as methylprednisolone (MP) and remyelinating neurosteroids such as allopregnanolone (ALLO) could be co-administered intranasally to enhance their efficacy by providing direct access to the central nervous system (CNS). **Methods:** The individual and combined effects of MP and ALLO to control the clinical score of murine experimental autoimmune encephalitis (EAE), to preserve spinal cord tissue integrity, modulate cellular infiltration and gliosis, promote remyelination, and modify the expression of Aryl hydrocarbon receptor (AhR) were evaluated. *In silico* studies, to deep insight into the mechanisms involved for the treatments, were also conducted. **Results:** MP was the only treatment that significantly reduced the EAE severity, infiltration of inflammatory cells and ionized calcium-binding adapter molecule 1 (*Iba-1*) expression respect to those EAE non-treated mice but with no-significant differences between the three treatments. MP, ALLO and MP+ALLO significantly reduced tissue damage, AhR expression, and promoted remyelination. Overall, these results suggest that MP, with or without the co-administration with ALLO is an effective and safe strategy to reduce the inflammatory status and the progression of EAE. Despite the expectations of the use of ALLO to reduce the inflammation in EAE, its effect in the dose-scheme used herein is limited only to improve myelination, an effect that supports its usefulness in demyelinating diseases. These results indicate the interest in exploring different doses of ALLO to recommend its use. **Conclusions:** ALLO treatment mainly maintain the integrity of the spinal cord tissue and the presence of myelin without affecting NI and the clinical outcome. AhR could be involved in the effect observed in both, MP and ALLO treatments. These results will help in the development of a more efficient therapy for MS patients.

Keywords: neuroinflammation; remyelination; allopregnanolone; methylprednisolone; AhR; glucocorticoids; neurosteroids; intranasal

1. Introduction

Multiple sclerosis (MS) a chronic autoimmune and demyelinating disease characterized by significant axonal injury and neuronal pathology, remains one of the leading causes of neurological disability in young adults, with increasing incidence and prevalence worldwide [1]. Relapsing-remitting multiple sclerosis (RRMS) is the most commonly diagnosed phenotype. It is characterized by recurrent episodes of Neuroinflammation (NI) and new lesions, with progressive loss of neurons and axons [2]. Currently, relapses in RRMS patients are treated with high doses of methylprednisolone (MP) administered orally or intravenously [3]. While it is known that effective con-

trol of NI favors recovery from MS relapses, recent evidence suggests that such control must be finely tuned. Indeed, myelin regeneration requires a delicate coordination between immune activation and regulation in complex interactive processes that are not yet fully understood [4].

Although MP reduces the severity of relapses and delays disease progression [5], the high doses required have adverse effects over time and may increase the risk of other morbidities [6]. To mitigate these drawbacks, the enhanced efficacy of intranasally administered MP for the treatment of MS relapses was demonstrated in a mouse model of experimental autoimmune encephalitis (EAE). Intranasally administered MP reduced EAE clinical scores and NI more effectively than the intravenous route [7]. These results are



consistent with previous reports that higher levels of dexamethasone were found in various brain regions of mice after intranasal (IN) administration of the steroid compared to intravenous administration. Similar results were observed when comparing MP administration by both routes assessed by immunofluorescence and high performance liquid chromatography (HPLC) analysis [8].

On the other hand, RRMS patients have low peripheral allopregnanolone (ALLO) levels that can be restored by the exogenous administration of this neurosteroid, that also exhibited anti-inflammatory properties and promote remyelination. Furthermore, ALLO has been shown to have some anti-inflammatory properties while promoting remyelination [9,10]. Here, the use of IN ALLO is proposed as a treatment to mitigate the progressive degenerative physiopathology associated to the EAE, alone or in combination with MP. Thus, we hypothesize that the addition of this neurosteroid, which is approved for human use in pathologies such as postpartum depression, could synergize the anti-inflammatory capacity of MP and promote myelin recovery in the EAE model as previously considered. Considering the higher efficiency of the IN route to reach the central nervous system (CNS) [7,8], we explore herein the usefulness of IN administration of ALLO.

Control of NI is not only critical in RRMS, but is also essential in numerous autoimmune diseases [11]. The Aryl hydrocarbon receptor (AhR), a ligand-activated transcription factor of the basic helix-loop-helix superfamily, has been proposed as a modulator of inflammation [12]. In addition, neuroactive steroid analogues of ALLO, such as $3\alpha,5\alpha$ -tetrahydrocorticosterone and $3\alpha,5\beta$ -tetrahydrocorticosterone, have been identified as endogenous AhR ligands with the ability to enhance the expression of myelinating glial cell markers and myelin-associated proteins, including myelin basic protein (MBP) [13]. AhR is also involved in the proliferation and differentiation of neural stem cells [14,15], plays a key role in the structure and maintenance of myelin [16], and regulates anti-inflammatory activity in peripheral immune cells and CNS resident cells [13]. Considering the above, the effects of ALLO and MP as ligands for this receptor were evaluated herein, and it was investigated whether their interactions modify AhR expression and its intracellular localization, particularly in neurons.

This study was aimed to evaluate the IN administration of MP plus ALLO as a therapeutic approach to control the severity of EAE and reduce the pathological outcome by controlling NI and promoting myelination.

2. Material and Methods

2.1 Animals

Mice were obtained from the animal facilities at the Instituto de Investigaciones Biomédicas (IIB), UNAM, Mexico City, Mexico. They were housed at the same institution

and maintained at 22 ± 3 °C with a 12/12 h light–dark cycle and with food and water (filtered, acidified, and sterilized) *ad libitum*.

All experimental procedures, including anesthesia and euthanasia, were conducted in accordance with national (NOM-062-ZOO-1999) and institutional regulations for the use and care of laboratory animals, following the protocol approved by the IIB, UNAM, Mexico (approval number ID 140).

The handling of the animals was carried out to minimize their suffering and stress. The animals were killed by administering a lethal dose of ketamine (100 mg/mL) and xylazine (100 mg/mL).

2.2 Experimental Autoimmune Encephalomyelitis Induction

EAE was induced in female mice as described previously [7]. Briefly, 14–16-week-old female C57BL/6J mice weighing at least 18 g were used. Mice were given *ad libitum* food and water before and during the experiments and were maintained under a 12:12 hours light/dark cycle. Each animal received 200 mg of a 1:1 emulsion of complete Freund's adjuvant (263910 and 231141, BD, Franklin Lakes, NJ, USA) and MOG35-55 peptide (LT12018, LifeTein, Somerset, NJ, USA) at 4 sites distributed along the dorsal flanks. Mice received an intraperitoneal dose of 300 ng pertussis toxin (180, Listlabs, Campbell, CA, USA) and a second dose of pertussis 48 hours later. Thereafter, mice weight, and clinical EAE score signs of each animal were measured daily until euthanized.

The clinical score was assessed by mice observation according to the criteria previously reported. Briefly, at clinical score zero (0) mice have no clinical signs, with normal gait and tail movement, tail can wrap around a round object if mouse is held at the base of the tail. At clinical score 1, mice have partially limp tail, with normal gait but the tip of the tail droops. At clinical score 2, mice have a paralyzed tail, with normal gait and complete tail drops. At clinical score 3, mice have hind limb paresis and uncoordinated movement, with uncoordinated gait, tail limps and hind limbs still respond to pinching (**Supplementary Table 1**). Complete clinical score criteria can be consulted at Bittner *et al.*, 2014 [17].

2.3 Treatments

All treatments were intranasally given following the protocol described by Hanson *et al.* [18]. In brief, mice were held, completely immobilizing the forelimbs and head with the non-dominant hand. While maintaining the grip on the scruff, the mice back was positioned on the holder palm and the chin was maintained as close as possible to a 180-degree angle. While each mouse was in this position, the treatments were administered using a 100 μ l micropipette (Eppendorf, Hamburg, Germany) making sure that the micropipette tip entered to the mouse nostril. For each mice

nostril, the total administered volume was 10 μ L, so the final volume in which each mouse treatment was dissolved was 40 μ L.

A commercially available formulation of methylprednisolone sodium succinate (Solumedrol, Pfizer, Manhattan, NY, USA) was administered at a concentration of 200 mg/kg as described elsewhere [7]. ALLO (PA STI 004670, Pharmaphilliates, Haryana, India) was administered at the reported optimal dose of 10 mg/kg diluted in sulfobutyl ether- β -cyclodextrin (Cat. RC-0C7-100, Captisol, Ligand Pharmaceuticals, San Diego, CA, USA) as previously described [19].

Two experiments with five groups of 3 to 6 mice each were performed. In each experiment groups were assigned as follows, naive mice group (naive), saline solution (SS) treated mice group (saline), MP treated mice group, ALLO treated mice group and MP+ALLO treated mice group. MP treated group received three doses of MP, which were administered for three consecutive days, when mice reached level two in the EAE clinical score, as previously described [7]. One (Fig. 1A) or six doses (Fig. 1B) of ALLO were administered on day 10 when mice had no symptoms, with or without the same MP dosage. Results shown in Figs. 2,3,4,5,6 correspond to the experiment shown in Fig. 1B.

2.4 Tissue Harvesting and Processing

Mice were euthanized on day 30 after EAE induction and tissues were stored for further processing. Briefly, mice were euthanized under deep anesthesia with ketamine and xylazine. Mice were bled and sera was collected and frozen at -80°C for cytokine quantification. Immediately after bled, mice were perfused transcardially with saline followed by 4% paraformaldehyde at 4°C to fix tissues. Spinal cord sections were obtained, and lumbar fractions were used for histological analysis by hematoxylin and eosin (H&E) staining or immunofluorescence (IF) labeling.

2.5 Histological Analysis

After dehydration and paraffin embedding, lumbar spinal cord fractions were cut into 5- μ m slices. Sections were deparaffinized in xylene, rehydrated in 100–75% gradient ethanol, and stained with H&E (Cat. ab245880, Abcam, Cambridge, UK) to characterize tissue damage. Images were acquired using a Leica DM500 microscope with a Leica ICC50 digital camera (Leica, Wetzlar, Germany). Sections were analyzed for tissue integrity and inflammatory infiltrate using Fiji, a distribution of the open-source software ImageJ 1.54i (National Institutes of Health (NIH), Bethesda, MD, USA) [20]. Briefly, tissue integrity was assessed by analyzing four areas per lumbar spinal cord section on photographs at 10x magnification. To analyze only the tissue contained on each photograph, the total tissue area of each section was delimited using the “Polygon Selection” tool [20]. Then, using the “Color Threshold” tool,

each photo was optimized for binary visualization, white for the tissue areas and black for non-tissue areas, making sure that the “Dark background” and “B&W” boxes were selected. Finally, the “Analyse Particles” tool [21] was used to measure the total stained and unstained areas. The unstained spaces, corresponding to the damaged tissue (black sections) were deployed in the “% area” column in the emergent window. The number of infiltrating cells was assessed by counting the stained nuclei in four areas per lumbar spinal cord section on photographs at 40x magnification with the “Multi-Point” tool of Fiji, which allows adding a small mark on counted nuclei.

2.6 Immunofluorescence

Upon fixation, lumbar spinal cord fractions were embedded in Tissue-Tek (Cat. DBK-4583, Dibbiotek, Mexico City, Mexico) for further cryo-sectioning using a Leica CM1860/CM1860 UV cryostat (Leica, Wetzlar, Hesse, Germany). Briefly, 20 μ m sections were preserved in phosphate-buffered saline solution (PBS) 1x until IF labeling, as reported elsewhere [7].

The following antibodies were used for immunostaining: *Iba1*, microglia and macrophage marker, 1:200 goat anti-Iba1 (ab5076, Abcam, Waltham, MA, USA) and 1:1000 donkey anti-goat Alexa Fluor 488 (ab150129, Abcam); glial fibrillary acidic protein (GFAP), astrocyte marker, 1:500 rabbit anti-GFAP (Z0334, Dako, Santa Clara, CA, USA) and 1:500 goat anti-rabbit Alexa Fluor 488 (A11008, ThermoFisher, Waltham, MA, USA); myelin basic protein (MBP): 1:500 rabbit anti-MBP (ab40390, Abcam) and 1:500 goat anti-rabbit Alexa Fluor 594 (A11012, ThermoFisher); myelin-associated glycoprotein (MAG): 1:500 rabbit anti-MAG (D4G3, Cell Signaling, Danvers, MA, USA) and 1:500 goat anti-rabbit Alexa Fluor 594 (A11012, ThermoFisher); AhR: 1:500 mouse anti-AhR (MA1-514, ThermoFisher) and 1:500 goat anti-mouse Alexa Fluor 488 (A28175, ThermoFisher); NeuN: 1:500 rabbit anti-NeuN (702022, ThermoFisher) and 1:500 goat anti-rabbit Alexa Fluor 594 (A11012, ThermoFisher). At the end of the incubation time, 4',6-diamidino-2-phenylindole (DAPI) (P3696, ThermoFisher) was added to each section to visualize nuclei.

Sections tissues analyzed by immunofluorescence were photographed using a Nikon AX/AX R confocal microscope (Nikon, Tokyo, Japan). Mean fluorescence intensity (MFI) analysis was performed using Fiji [19]. Briefly, for each analyzed photograph, the “Split Channels” tool was used to separate color channels, and the selected marker labeling was analyzed. Then, the “Measure” tool was used to assign the MFI value for each photograph, which corresponds to the “Mean” value in the resulting emergent window.

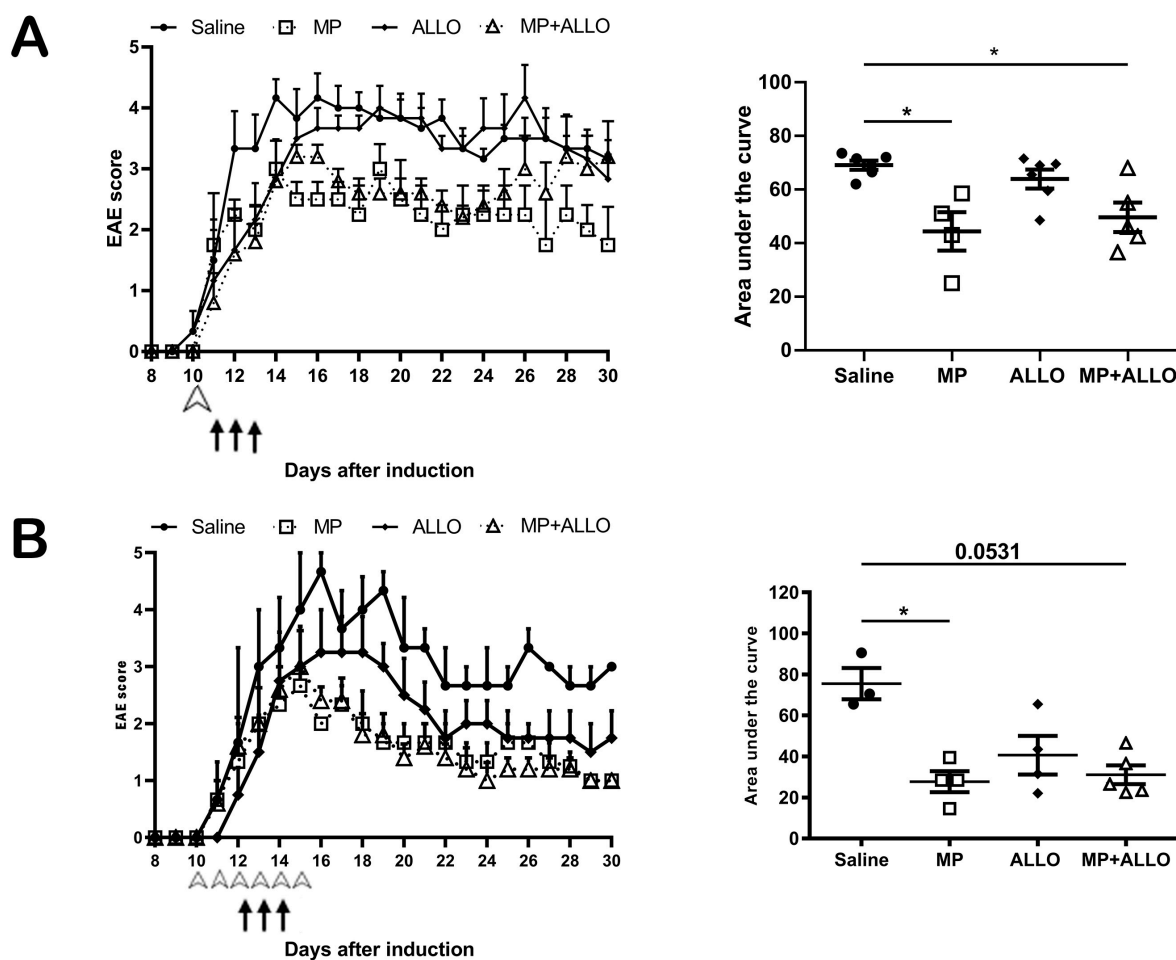


Fig. 1. EAE clinical score of mice from two experiments. (A) Daily recording of EAE clinical score in treated and non-treated mice. White arrow points a single dose of ALLO 10 days after EAE induction, while the black arrows point a three-day administration of MP, the same administration scheme was used for the MP+ALLO group. (B) Daily recording of EAE clinical score in treated and non-treated mice. White arrow points a six-day dose of ALLO 10 days after EAE induction, while the black arrows point a three-day administration of MP, the same administration scheme was used for the MP+ALLO group. For A and B, three to five mice were included in each group, error bars indicate SEM, $*p < 0.05$. EAE, experimental autoimmune encephalitis; ALLO, allopregnanolone; MP, methylprednisolone; SEM, standard error of the mean.

2.7 Molecular Docking

The molecular structure of *Mus musculus* AhR was obtained from Protein Data Bank [22]. Both MP and ALLO structures were obtained from PubChem (MP PubChem CID 23680530, ALLO PubChem CID 92786). For molecular docking analysis and docking reconstruction images, blind docking was performed using the online molecular docking tools CB-DOCK and CB-DOCK2 (<http://clab.labshare.cn/cb-dock/> and <https://cadd.labshare.cn/cb-dock2/index.php>) following the procedure previously reported [23,24].

2.8 Colocalization Analysis

The colocalization of NeuN+/AhR+ was performed using the “JACoP” and “Colocalization Finder” plugins [25]. Briefly, on each analyzed section, the color channels were separated so that the green (AhR+) and red (NeuN+)

channels could be visualized individually. Subsequently, the “JACoP” plugin was used to calculate the Pearson’s correlation coefficient, while the “Collocation Finder” plugin was used to generate the scatter plots corresponding to each section.

2.9 Statistical Analysis

Data were first tested for a normal distribution using the Kolmogorov and Smirnov test and tested for homogeneity of variance using Bartlett’s method. If data were normally distributed, one-way Analysis of Variance (ANOVA) was used with a post hoc Tukey test. If data were not normally distributed, non-parametric Kruskal-Wallis Test (Nonparametric ANOVA) was used and the statistically significant differences between groups were estimated using the Unpaired *t* test with Welch correction.

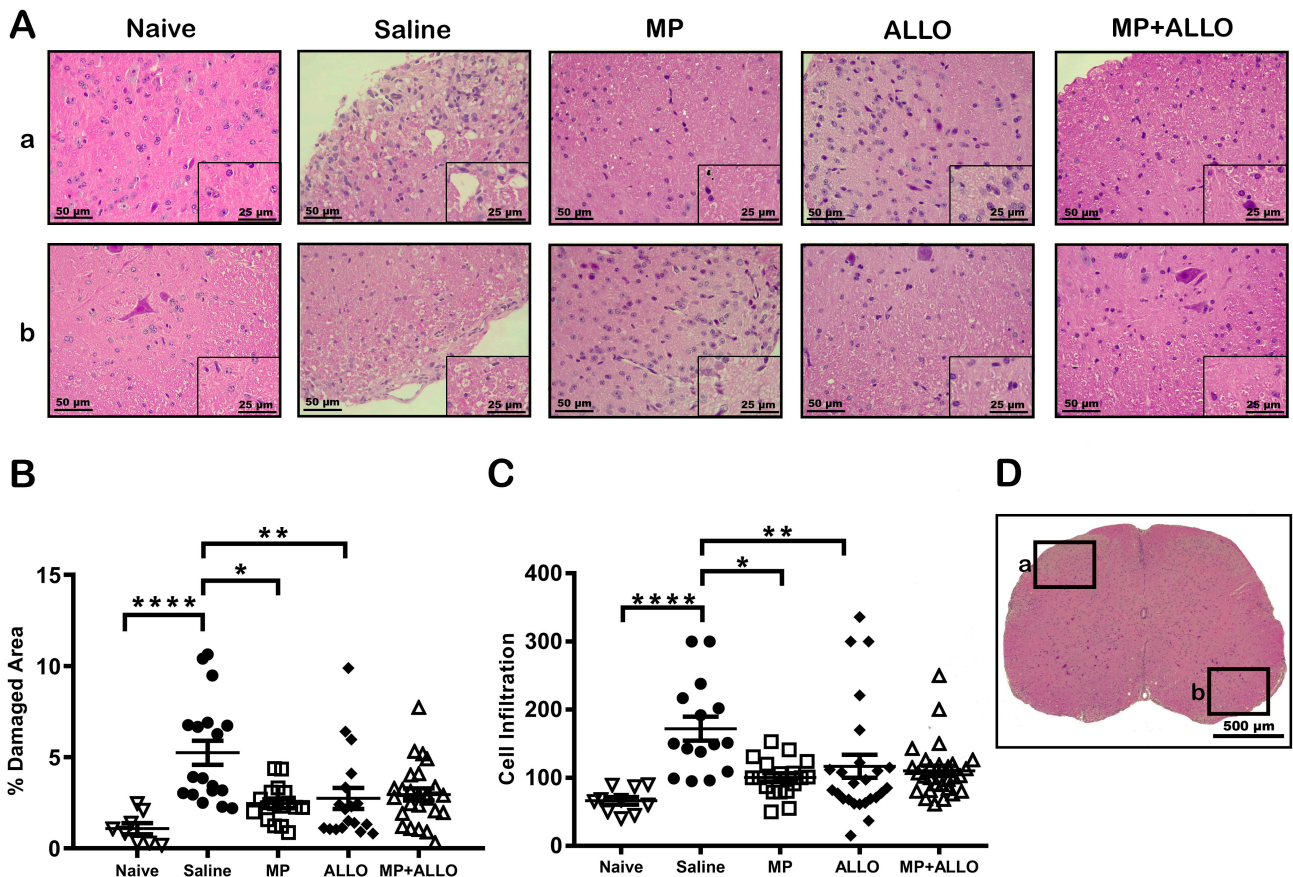


Fig. 2. Histologic analysis of lumbar spinal cord sections. (A) Representative images of the analyzed areas of different zones (a and b) highlighted at D (Black squares pointing different areas in the lumbar spinal cord sections). MP, ALLO and MP+ALLO treatments diminished the EAE effect on the tissue integrity and the inflammatory cellular infiltrate. Scale bars, 50 μ m and 25 μ m (A) and 500 μ m (D). (B,C) Mean of damaged area and cell infiltration in 3 to 6 mice from each group. Analyzed data corresponds to the experiment showed in Fig. 1B, for each group, according to the availability of the material 2 to 4 sections were analyzed, naive n = 4, saline n = 3, MP n = 4, ALLO n = 4, MP+ALLO n = 5, Kruskal-Wallis Test and for group differences an unpaired *t* test with Welch correction, error bars indicate SEM, **p* < 0.05, ***p* < 0.01, *****p* < 0.0001.

All statistical analyses were performed with Prism 8.0 (GraphPad Software Inc., San Diego, CA, USA). Results were considered statistically significant at $p \leq 0.05$.

3. Results

In a previous study, Rassy *et al.* (2020) [7] demonstrated that MP intranasally administered reduced signs of EAE more effectively than the intravenous route. The effect of IN administration of MP and ALLO, both individually and in combination, was evaluated herein. As shown in Fig. 1A,B, MP and MP+ALLO treatments significantly reduced the clinical EAE score compared to the saline-treated group. Meanwhile, ALLO treatment only tends to diminish the EAE score.

The lumbar region of the spinal cord was analyzed since it is the most affected region in EAE. As shown in Fig. 2A, the induction of the model significantly increased cellular infiltration and the percentage of damage areas. The three treatments reduced the size of the damaged areas,

but cellular infiltration was significantly reduced only in the lumbar section of animals treated with MP and MP+ALLO.

The expression levels of *GFAP* and *Iba1* in astrocytes and microglia, respectively, are considered indicators of glial activation. As shown in Fig. 3, treatment with MP and MP+ALLO significantly reduced the MFI values of *GFAP* compared to saline-treated mice. *Iba1* expression was significantly reduced only in MP-treated animals.

Loss of the myelin sheath is a hallmark in EAE. As shown in Fig. 4, all treatments induced recovery of *MBP* and *MAG* expression, both structural components of myelin. A slightly higher effect was induced in ALLO- and MP+ALLO-treated mice.

To evaluate if differences in decreasing severity by the two steroids tested, the possible participation of the level of receptors expressed was evaluated. As shown in Fig. 5A,B, both MP and ALLO increase the expression of AhR to a similar extend, a receptor involved in myelination and the regulation of inflammation. This increase could be resulted

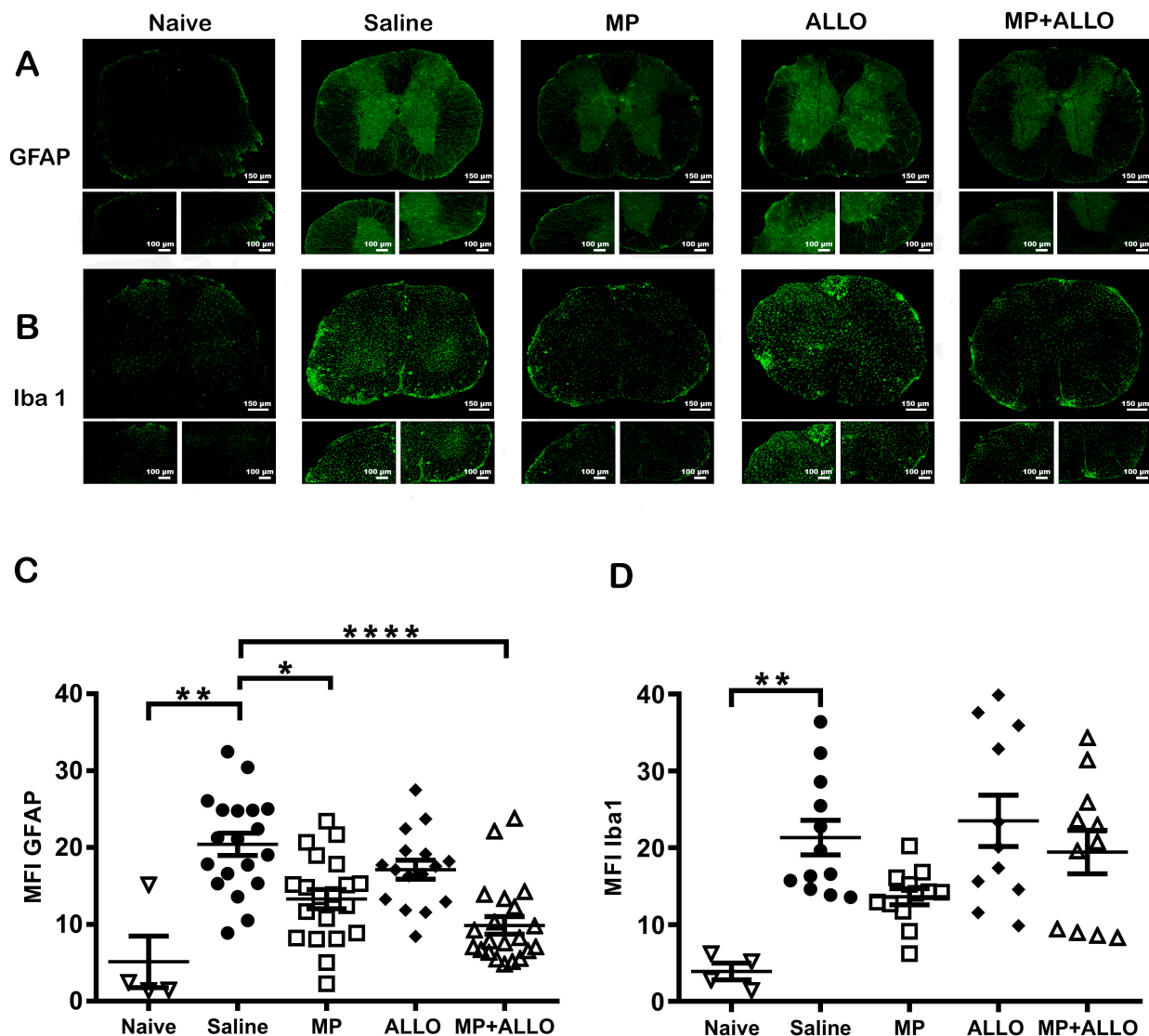


Fig. 3. GFAP and Iba1 expression. (A,B) Lumbar spinal cord sections photographs (20x and 40x). Scale bars, 150 μm and 100 μm respectively. (C,D) Mean MFI of GFAP and Iba1 expression in spinal cord sections in 3 to 6 mice from each group. Analyzed data corresponds to the experiment showed in Fig. 1B, for each group, according to the availability of the material 2 to 4 sections were analyzed, naive n = 4, SS n = 3, MP n = 4, ALLO n = 4, MP+ALLO n = 5, for GFAP Kruskal-Wallis Test and for group differences an unpaired *t* test with Welch correction, for Iba1 One-way ANOVA with post hoc Tukey test, error bars indicate SEM, **p* < 0.05, ***p* < 0.01, ****p* < 0.0001. GFAP, Glial fibrillary acidic protein; Iba1, ionized calcium-binding adapter molecule 1.

by interaction of MP and ALLO with this receptor, a feature supported by the theoretical predictions when both drugs are structurally compared with 2,3,7,8-Tetrachlorodibenzo-p-dioxin (TCDD), also known as dioxin, that is a potent agonist of AhR (Fig. 5C,D).

AhR has been reported to have different functions depending on the type of cells and its location, either cytoplasmic or nuclear. As shown in Fig. 6, all treatments promoted nuclear translocation of AhR in neurons as measured by its colocalization with NeuN, a neuronal nuclear marker. It can also be observed that EAE decreased AhR nuclear translocation.

4. Discussion

MP has been recognized as an effective alternative to reduce the pathological signs in MS and EAE (a well-studied RRMS model), by reducing immune cell infiltration and demyelination [7]. It is also known that ALLO expression is downregulated in RRMS adult patients [10,26], a neurosteroid involved in the myelination in the CNS [9]. On the other hand, we previously demonstrated that the IN route is more effective than the intravenous to reach the CNS [8]. Based on this information, herein the evaluation of the efficacy of IN administration of MP and ALLO, alone and in combination, was performed to control EAE pathologic signs.

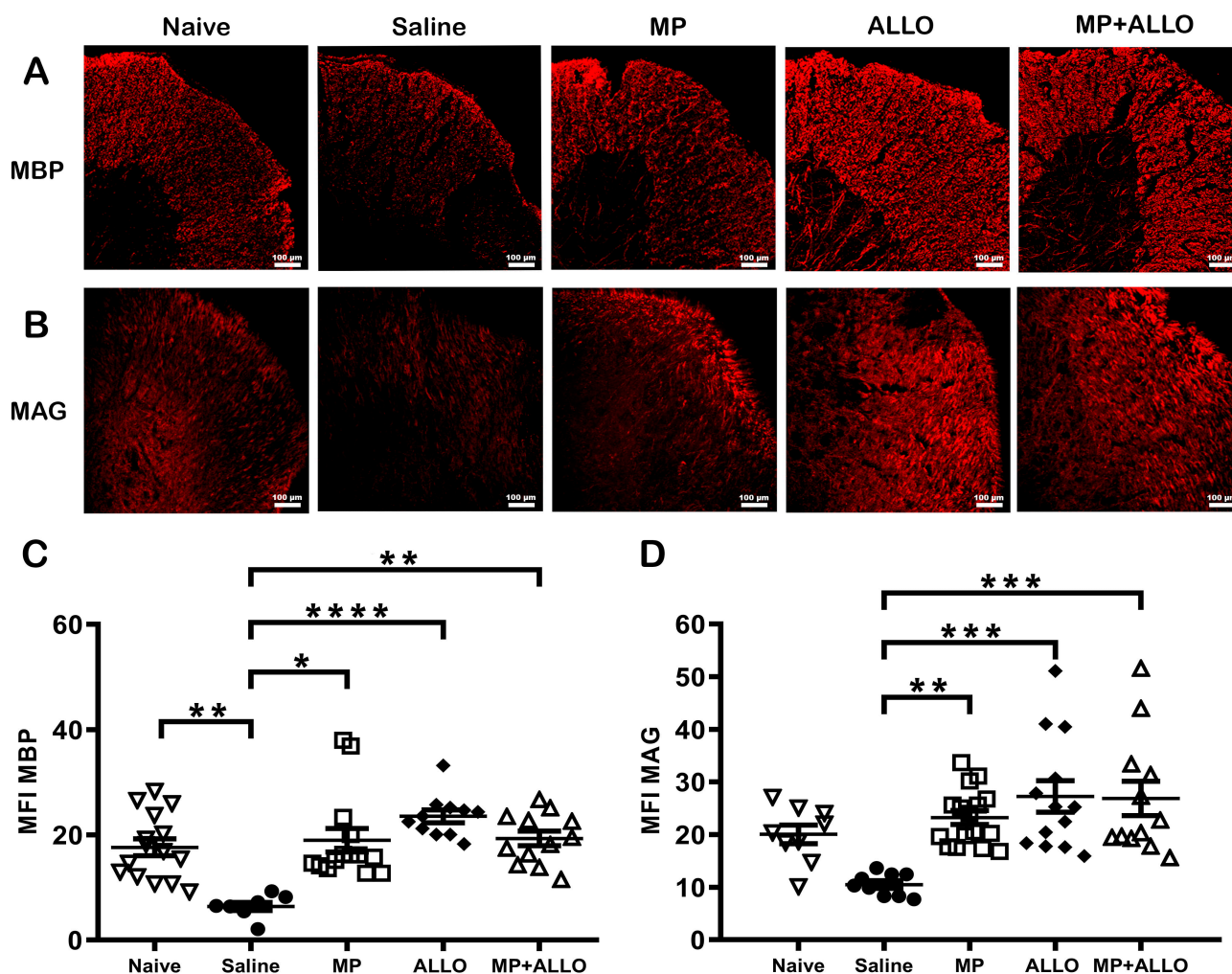


Fig. 4. Expression of *MBP* and *MAG* in lumbar spinal cord sections. (A,B) Micrographs of spinal cord sections at 20x magnification. MP, ALLO and MP+ALLO treatments rise the expression of *MBP* and *MAG* in comparison to the SS treated group. Scale bar, 100 µm. (C,D) MFI of *MBP* and *MAG* expression in spinal cord sections in 3 to 6 mice from each group. Analyzed data corresponds to the experiment showed in Fig. 1B, for each group, according to the availability of the material 2 to 4 sections were analyzed, nave n = 4, SS n = 3, MP n = 4, ALLO n = 4, MP+ALLO n = 5. *MBP* data were compared using the Kruskal-Wallis Test followed by the unpaired *t* test with Welch correction. *MAG* data were analyzed using the one-way ANOVA with post hoc Tukey test. Mean of the MFI was included with an error bar that indicates the SEM, **p* < 0.05, ***p* < 0.01, ****p* < 0.001, *****p* < 0.0001. MBP, myelin basic protein; MFI, mean fluorescence intensity; MAG, myelin-associated glycoprotein.

Consistent with previous results [7], MP intranasally administered effectively reduced the peak value of clinical scores in two independent experiments performed (Fig. 1). ALLO alone did not affect the clinical score in EAE mice, but used in combination with MP, did not diminish the beneficial effect of the latter, used before or after the appearance of the symptoms neither at one nor at six doses administered. The absence of effect on clinical outcomes induced by ALLO is compatible with its lower anti-inflammatory capacity relative to the high potency of MP [27–29]. Indeed, MP effectively controlled the cellular infiltration and down-regulate the gliosis induced in EAE control mice [30,31]. Gliosis, directly involved in RRMS progression [32], is characterized by activation of astrocytes and mi-

croglia that overexpressed *GFAP* and *Iba1*, respectively [33–37]. The lack of effect of ALLO on the clinical improvement of the mice is accompanied by a sustained inflammation that is manifested by the maintenance of the increased inflammatory infiltrate in EAE together with the increased levels of astrocytes and microglia activation. However, Noorbakhsh *et al.* 2011 [26], reported the effectiveness of ALLO daily administered for 30 days, from the induction of the model to the euthanasia of the animals, in controlling the clinical score in EAE mice. This sustained schedule probably compensates for the lower anti-inflammatory capacity of ALLO, allowing the clinical improvement of mice.

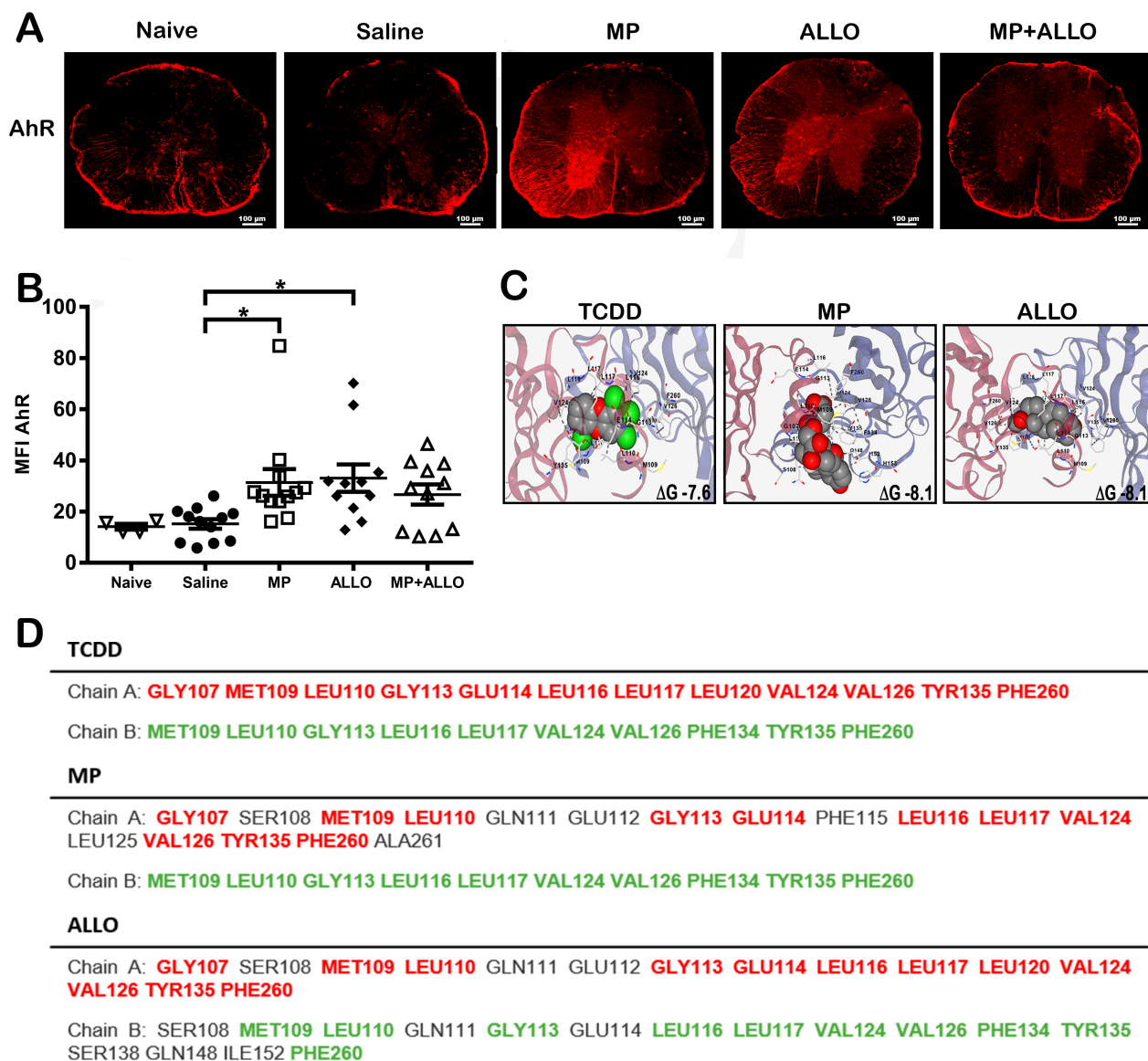


Fig. 5. AhR expression and ligand interactions. (A) AhR expression in spinal cord sections. MP, ALLO and MP+ALLO treatments rise the expression of AhR in comparison to the SS treated group. Scale bar, 100 μ m. (B) MFI analysis of AhR expression in spinal cord sections in 3 to 6 mice from each group. Analyzed data corresponds to the experiment showed in Fig. 1B, for each group, according to the availability of the material 2 to 4 sections were analyzed, naive n = 4, saline n = 3, MP n = 4, ALLO n = 4, MP+ALLO n = 5, Kruskal-Wallis Test and for group differences an unpaired *t* test with Welch correction, error bars indicate SEM, **p* < 0.05. (C) Potential interactions between AhR and different ligands analyzed by molecular docking. Both MP and ALLO have greater binding free energy than TCDD, the gold standard AhR ligand. (D) Comparison of interacting amino acids of AhR with TCDD, MP and ALLO. Red and green letters indicate common interacting amino acids in AhR between TCDD, MP and ALLO. Black lettering indicates amino acids that interact only with MP or ALLO. AhR, Aryl hydrocarbon receptor. TCDD, 2,3,7,8-Tetrachlorodibenzop-dioxin.

Despite the low anti-inflammatory capacity of ALLO, it could reduce the areas of damage in the spinal cord and increase the level of the expression of the Aryl receptor and myelin expression. This profile is compatible with the capacity of ALLO to modulate the specific immunity elicited against myelin in EAE that could be overridden by the sustained increased global inflammation. This possibility must be further explored.

Another point that merit comments are the possible effects of steroids and neurosteroids on oligodendrocytes. These cells produce myelin, the protein that wraps around nerve fibers essential to promote signal transmission. Under neuroinflammatory conditions, that prevail in MS and EAE, oligodendrocytes become dysfunctional, leading to myelin damage and axonal degeneration, that affect white and grey matter of the CNS. Under pathological conditions

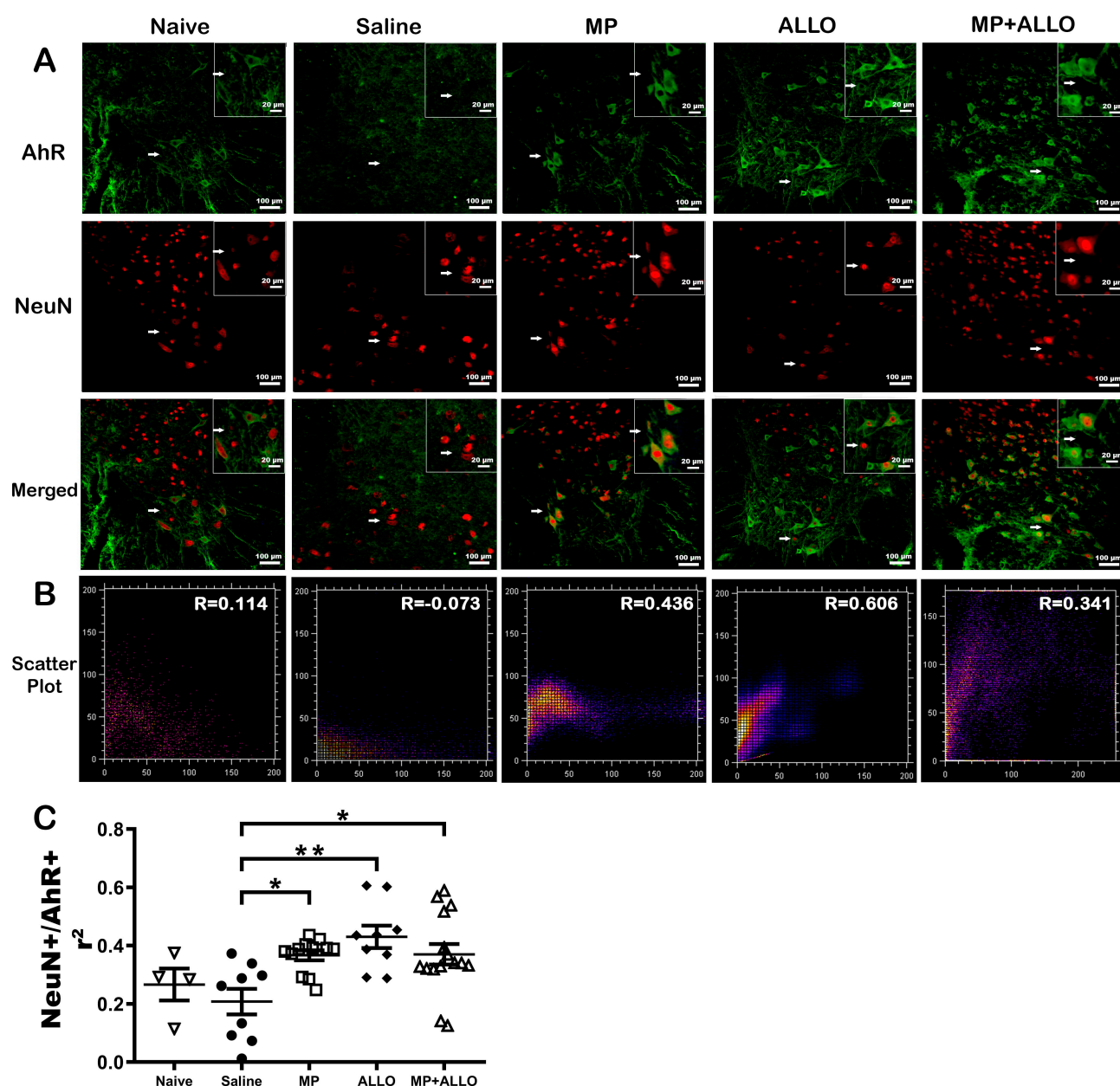


Fig. 6. Colocalization of NeuN and AhR. (A) Micrographs of spinal cord sections at 40x and 60x magnification. Green AhR expression, red NeuN expression and blue DAPI. MP, ALLO and MP+ALLO treatments promoted the colocalization of AhR and NeuN, compared to the SS treated group. Scale bars, 100 μ m and 20 μ m respectively. (B) Scatter plot of AhR and NeuN colocalization. (C) Analysis of AhR and NeuN colocalization by Pearson's Correlation analysis in spinal cord sections in 3 to 6 mice from each group. Analyzed data corresponds to the experiment showed in Fig. 1B, for each group, according to the availability of the material 2 to 4 sections were analyzed, naive n = 4, SS n = 3, MP n = 4, ALLO n = 4, MP+ALLO n = 5, One-way ANOVA with post hoc Tukey test, error bars indicate SEM, * p < 0.05, ** p < 0.01. NeuN, neuron specific nuclear protein; DAPI, 4',6-diamidino-2-phenylindole.

such as demyelinating injury, several neuroactive steroids, including ALLO, have shown remyelinating effects [38]. In this study the possibility of myelin regeneration by treatment with MP and/or ALLO was investigated. We found increased expression levels of the *MBP* and *MAG*, more significantly in mice treated with ALLO than with MP. The effective anti-inflammatory capacity of MP may favor the increase level of the expression of both myelin proteins.

On the other hand, the remyelinating effect of ALLO could be mediated by its interaction with *aminobutyric acid receptors A* (GABAA) receptors expressed in precursor and mature myelinating cells since it occurs on an exacerbated cellular infiltration and gliosis, a finding that point to the potential utility of ALLO as a therapy to improve RRMS patients.

It has been reported that the deletion of AhR, a highly conserved receptor expressed on a variety of cells, including resident CNS cells such as oligodendrocytes, astrocytes, microglia, and neurons [39,40], expressed in microglia inhibit the remyelination [41]. In addition, in the CNS, AhR has been implicated in the modulation of NI, cell proliferation, and myelination [14–16,42]. Considering that AhR receptors could be involved in the increase of myelin proteins induced by both steroids [41,43], the outcome of the treatments on the expression of AhR was tested. The three treatments, MP, ALLO and MP+ALLO, increased AhR expression to a similar extent, that could be due to their high affinity observed in the molecular docking analysis (Fig. 5), which is even higher than its specific agonist TCDD. On the other hand, several functions of AhR have been described in CNS resident cells, depending on whether AhR is expressed in the cytoplasm or in the nucleus [44]. As shown in Fig. 6, EAE induction inhibited AhR translocation to the nucleus of spinal cord neurons, a finding that is accompanied by the reduced levels of *MBP* and *MAG* in untreated or saline-treated mice that can be counteracted by ALLO administration even more effective than the other treatments. This nuclear translocation could be mediated by the *GABAergic* pathway, that has been reported to trigger remyelinating communication between neurons and oligodendrocyte precursor cells [45]. Indeed, several reports support our findings and highlight the beneficial effects of AhR overexpression and activation in demyelinating pathologies. It is worthy to mention that AhR depletion or downregulation of its expression promotes not only NI, but also demyelinating pathologies, locomotor defects, and altered myelin structure [16,43]. Overall, our findings sustained that AhR could contribute to the myelinating effects induced by both MP and ALLO, while the effective anti-inflammatory properties of MP could favor the induced remyelination.

5. Conclusions

This study highlights the efficacy of MP intranasally administered to effectively control the NI reducing the severity of EAE pathology in mice, whilst IN ALLO treatment mainly maintain the integrity of the spinal cord tissue and the presence of myelin without affecting NI and the clinical outcome. Different mechanisms could underlie the MP and ALLO effects on EAE, but part of them could be mediated by the increased expression of AhR, a receptor that has been reported to have multiple functions under different physiological and pathological conditions whose participation merit to be further explored. These results will help in the development of a more efficient therapy for MS patients.

Availability of Data and Materials

Data and imaging of the datasets generated in this study are available from the corresponding authors on reasonable request.

Author Contributions

ES, GF, HB, and MATR designed the study. CAG, RGF, JAEC, and INPO performed the research. ES, CAG, and INPO analyzed data. ES, GF, MATR, and INPO drafted the manuscript. All authors have participated sufficiently in the work to take public responsibility for appropriate portions of the content and agreed to be accountable for all aspects of the work in ensuring that questions related to its accuracy or integrity. All authors contributed to editorial changes in the manuscript. All authors read and approved the final manuscript.

Ethics Approval and Consent to Participate

All experimental procedures involving animals were approved by the Institutional Care and Animal Use Committee (CICUAL, protocol ID 140) at the IIB-UNAM, following the Mexican regulation (NOM 062-ZOO-1999) and in accordance with the recommendations from the National Institute of Health of the USA (Guide for the Care and Use of Laboratory Animals).

Acknowledgment

We gratefully acknowledge PhD Marisela Hernandez, Gonzalo Acero and MVZ Georgina Dıaz Herrera for her technical support and to the “Unidad de Modelos Biologicos” of the IIB, UNAM, Mexico for animal lodging and handling. Also, we acknowledge the CONAHcyT Grant 3004601 to INNMMVS for the confocal microscope facilities usage.

Funding

This research was funded by the Consejo Nacional de Humanidades, Ciencias y Tecnologıas: CY002261 FRONTERAS, Direccion General de Personal Academico, UNAM: PAPIIT IN207720, IN211823; the Institutional Program “Programa de Investigacion para el Desarrollo y la Optimizacion de Vacunas, Inmunomoduladores y Metodos Diagnosticos del IIBO” (PROVACADI, UNAM).

Conflict of Interest

The authors declare no conflict of interest.

Supplementary Material

Supplementary material associated with this article can be found, in the online version, at <https://doi.org/10.31083/j.fbl2912420>.

References

- [1] Jakimovski D, Bittner S, Zivadinov R, Morrow SA, Benedict RH, Zipp F, *et al.* Multiple sclerosis. *Lancet* (London, England). 2024; 403: 183–202. [https://doi.org/10.1016/S0140-6736\(23\)01473-3](https://doi.org/10.1016/S0140-6736(23)01473-3).
- [2] Tagge IJ, Leppert IR, Fetco D, Campbell JS, Rudko DA, Brown RA, *et al.* Permanent tissue damage in multiple sclerosis lesions is associated with reduced pre-lesion myelin and

- axon volume fractions. *Multiple Sclerosis* (Houndmills, Basingstoke, England). 2022; 28: 2027–2037. <https://doi.org/10.1177/13524585221110585>.
- [3] Le Page E, Veillard D, Laplaud DA, Hamonic S, Wardi R, Lebrun C, *et al.* Oral versus intravenous high-dose methylprednisolone for treatment of relapses in patients with multiple sclerosis (COPOUSEP): a randomised, controlled, double-blind, non-inferiority trial. *Lancet* (London, England). 2015; 386: 974–981. [https://doi.org/10.1016/S0140-6736\(15\)61137-0](https://doi.org/10.1016/S0140-6736(15)61137-0).
 - [4] Franklin RJM, Simons M. CNS remyelination and inflammation: From basic mechanisms to therapeutic opportunities. *Neuron*. 2022; 110: 3549–3565. <https://doi.org/10.1016/j.neuron.2022.09.023>.
 - [5] Saied A, Elsaid N, Azab A. Long term effects of corticosteroids in multiple sclerosis in terms of the “no evidence of disease activity” (NEDA) domains. *Steroids*. 2019; 149: 108401. <https://doi.org/10.1016/j.steroids.2019.04.006>.
 - [6] Ömerhoca S, Haşimoğlu ZY, Erdoğan S, Kale N. The Adverse Effects of High-Dose Corticosteroids with Early and Late Severe Morbidity in the Treatment of Patients with Multiple Sclerosis: Long-Term Observation Results. *Turkish Journal of Neurology*. 2019; 25: 71–75. <https://doi.org/10.4274/tnd.2019.75725>.
 - [7] Rassy D, Bárcena B, Pérez-Osorio IN, Espinosa A, Peón AN, Terrazas LI, *et al.* Intranasal Methylprednisolone Effectively Reduces Neuroinflammation in Mice with Experimental Autoimmune Encephalitis. *Journal of Neuropathology and Experimental Neurology*. 2020; 79: 226–237. <https://doi.org/10.1093/jnen/nl128>.
 - [8] Pérez-Osorio IN, Espinosa A, Giraldo Velázquez M, Padilla P, Bárcena B, Fragoso G, *et al.* Nose-to-Brain Delivery of Dexamethasone: Biodistribution Studies in Mice. *The Journal of Pharmacology and Experimental Therapeutics*. 2021; 378: 244–250. <https://doi.org/10.1124/jpet.121.000530>.
 - [9] Diviccaro S, Cioffi L, Falvo E, Giatti S, Melcangi RC. Allopregnanolone: An overview on its synthesis and effects. *Journal of Neuroendocrinology*. 2022; 34: e12996. <https://doi.org/10.1111/jne.12996>.
 - [10] Noorbakhsh F, Baker GB, Power C. Allopregnanolone and neuroinflammation: a focus on multiple sclerosis. *Frontiers in Cellular Neuroscience*. 2014; 8: 134. <https://doi.org/10.3389/fncel.2014.00134>.
 - [11] Altmann DM. Neuroimmunology and neuroinflammation in autoimmune, neurodegenerative and psychiatric disease. *Immunology*. 2018; 154: 167–168. <https://doi.org/10.1111/imm.12943>.
 - [12] Dai S, Qu L, Li J, Zhang Y, Jiang L, Wei H, *et al.* Structural insight into the ligand binding mechanism of aryl hydrocarbon receptor. *Nature Communications*. 2022; 13: 6234. <https://doi.org/10.1038/s41467-022-33858-w>.
 - [13] Wu PY, Chuang PY, Chang GD, Chan YY, Tsai TC, Wang BJ, *et al.* Novel Endogenous Ligands of Aryl Hydrocarbon Receptor Mediate Neural Development and Differentiation of Neuroblastoma. *ACS Chemical Neuroscience*. 2019; 10: 4031–4042. <https://doi.org/10.1021/acscchemneuro.9b00273>.
 - [14] Dever DP, Adham ZO, Thompson B, Genestine M, Cherry J, Olschowka JA, *et al.* Aryl hydrocarbon receptor deletion in cerebellar granule neuron precursors impairs neurogenesis. *Developmental Neurobiology*. 2016; 76: 533–550. <https://doi.org/10.1002/dneu.22330>.
 - [15] Imran SJ, Vagaska B, Kriska J, Anderova M, Bortolozzi M, Gerosa G, *et al.* Aryl Hydrocarbon Receptor (AhR)-Mediated Signaling in iPSC-Derived Human Motor Neurons. *Pharmaceuticals* (Basel, Switzerland). 2022; 15: 828. <https://doi.org/10.3390/ph15070828>.
 - [16] Juricek L, Carcaud J, Pelhaitre A, Riday TT, Chevallier A, Lanzini J, *et al.* AhR-deficiency as a cause of demyelinating disease and inflammation. *Scientific Reports*. 2017; 7: 9794. <https://doi.org/10.1038/s41598-017-09621-3>.
 - [17] Bittner S, Afzali AM, Wiendl H, Meuth SG. Myelin oligodendrocyte glycoprotein (MOG35-55) induced experimental autoimmune encephalomyelitis (EAE) in C57BL/6 mice. *Journal of Visualized Experiments: JoVE*. 2014; 51275. <https://doi.org/10.3791/51275>.
 - [18] Hanson LR, Fine JM, Svitak AL, Faltese KA. Intranasal administration of CNS therapeutics to awake mice. *Journal of Visualized Experiments: JoVE*. 2013; 4440. <https://doi.org/10.3791/4440>.
 - [19] Zolkowska D, Wu CY, Rogawski MA. Intranasal Allopregnanolone Confers Rapid Seizure Protection: Evidence for Direct Nose-to-Brain Delivery. *Neurotherapeutics: the Journal of the American Society for Experimental NeuroTherapeutics*. 2021; 18: 544–555. <https://doi.org/10.1007/s13311-020-00985-5>.
 - [20] Schindelin J, Arganda-Carreras I, Frise E, Kaynig V, Longair M, Pietzsch T, *et al.* Fiji: an open-source platform for biological-image analysis. *Nature Methods*. 2012; 9: 676–682. <https://doi.org/10.1038/nmeth.2019>.
 - [21] Rishi K, Rana N. Particle Size and Shape Analysis Using ImageJ with Customized Tools for Segmentation of Particles. *International Journal of Engineering Research & Technology*. 2015; 4: 247–250. <https://www.ijert.org/particle-size-and-shape-analysis-using-imagej-with-customized-tools-for-segmentation-of-particles>.
 - [22] Wu D, Potluri N, Kim Y, Rastinejad F. Structure and dimerization properties of the aryl hydrocarbon receptor PAS-A domain. *Molecular and Cellular Biology*. 2013; 33: 4346–4356. <https://doi.org/10.1128/MCB.00698-13>.
 - [23] Liu Y, Grimm M, Dai WT, Hou MC, Xiao ZX, Cao Y. CB-Dock: a web server for cavity detection-guided protein-ligand blind docking. *Acta Pharmacologica Sinica*. 2020; 41: 138–144. <https://doi.org/10.1038/s41401-019-0228-6>.
 - [24] Liu Y, Yang X, Gan J, Chen S, Xiao ZX, Cao Y. CB-Dock2: improved protein-ligand blind docking by integrating cavity detection, docking and homologous template fitting. *Nucleic Acids Research*. 2022; 50: W159–W164. <https://doi.org/10.1093/nar/gkac394>.
 - [25] Bolte S, Cordelières FP. A guided tour into subcellular colocalization analysis in light microscopy. *Journal of Microscopy*. 2006; 224: 213–232. <https://doi.org/10.1111/j.1365-2818.2006.01706.x>.
 - [26] Noorbakhsh F, Ellestad KK, Maingat F, Warren KG, Han MH, Steinman L, *et al.* Impaired neurosteroid synthesis in multiple sclerosis. *Brain: a Journal of Neurology*. 2011; 134: 2703–2721. <https://doi.org/10.1093/brain/awr200>.
 - [27] Balan I, Boero G, Chéry SL, McFarland MH, Lopez AG, Morrow AL. Neuroactive Steroids, Toll-like Receptors, and Neuroimmune Regulation: Insights into Their Impact on Neuropsychiatric Disorders. *Life* (Basel, Switzerland). 2024; 14: 582. <https://doi.org/10.3390/life14050582>.
 - [28] Samuel S, Nguyen T, Choi HA. Pharmacologic Characteristics of Corticosteroids. *Journal of Neurocritical Care*. 2017; 10: 53–59. <https://doi.org/10.18700/jnc.170035>.
 - [29] Coutinho AE, Chapman KE. The anti-inflammatory and immunosuppressive effects of glucocorticoids, recent developments and mechanistic insights. *Molecular and Cellular Endocrinology*. 2011; 335: 2–13. <https://doi.org/10.1016/j.mce.2010.04.005>.
 - [30] Li L, Xu Q, Wu Y, Hu W, Gu P, Fu Z. Combined therapy of methylprednisolone and brain-derived neurotrophic factor promotes axonal regeneration and functional recovery after spinal cord injury in rats. *Chinese Medical Journal*. 2003; 116: 414–418.
 - [31] Liu WL, Lee YH, Tsai SY, Hsu CY, Sun YY, Yang LY, *et*

- al.* Methylprednisolone inhibits the expression of glial fibrillary acidic protein and chondroitin sulfate proteoglycans in reactivated astrocytes. *Glia*. 2008; 56: 1390–1400. <https://doi.org/10.1002/glia.20706>.
- [32] Popescu BFG, Pirkó I, Lucchinetti CF. Pathology of multiple sclerosis: where do we stand? *Continuum (Minneapolis, Minn.)*. 2013; 19: 901–921. <https://doi.org/10.1212/01.CON.0000433291.23091.65>.
- [33] Lafrenaye AD, Mondello S, Wang KK, Yang Z, Povlishock JT, Gorse K, *et al.* Circulating GFAP and Iba-1 levels are associated with pathophysiological sequelae in the thalamus in a pig model of mild TBI. *Scientific Reports*. 2020; 10: 13369. <https://doi.org/10.1038/s41598-020-70266-w>.
- [34] Grimaldi A, Pediconi N, Oieni F, Pizzarelli R, Rosito M, Giubertini M, *et al.* Neuroinflammatory Processes, A1 Astrocyte Activation and Protein Aggregation in the Retina of Alzheimer's Disease Patients, Possible Biomarkers for Early Diagnosis. *Frontiers in Neuroscience*. 2019; 13: 925. <https://doi.org/10.3389/fnins.2019.00925>.
- [35] Abdelhak A, Foschi M, Abu-Rumeileh S, Yue JK, D'Anna L, Huss A, *et al.* Blood GFAP as an emerging biomarker in brain and spinal cord disorders. *Nature Reviews. Neurology*. 2022; 18: 158–172. <https://doi.org/10.1038/s41582-021-00616-3>.
- [36] Peng W, Xie Y, Liao C, Bai Y, Wang H, Li C. Spatiotemporal patterns of gliosis and neuroinflammation in presenilin 1/2 conditional double knockout mice. *Frontiers in Aging Neuroscience*. 2022; 14: 966153. <https://doi.org/10.3389/fnagi.2022.966153>.
- [37] Jurga AM, Paleczna M, Kuter KZ. Overview of General and Discriminating Markers of Differential Microglia Phenotypes. *Frontiers in Cellular Neuroscience*. 2020; 14: 198. <https://doi.org/10.3389/fncel.2020.00198>.
- [38] Kalakh S, Mouihate A. The Effects of Neuroactive Steroids on Myelin in Health and Disease. *Medical Principles and Practice: International Journal of the Kuwait University, Health Science Centre*. 2024; 33: 198–214. <https://doi.org/10.1159/000537794>.
- [39] Barroso A, Mahler JV, Fonseca-Castro PH, Quintana FJ. The aryl hydrocarbon receptor and the gut-brain axis. *Cellular & molecular immunology*. 2021; 18: 259–268. <https://doi.org/10.1038/s41423-020-00585-5>.
- [40] Juricek L, Coumoul X. The Aryl Hydrocarbon Receptor and the Nervous System. *International Journal of Molecular Sciences*. 2018; 19: 2504. <https://doi.org/10.3390/ijms19092504>.
- [41] Wang Y, Sun J, Zhu K, Wang D, Zhao X, Zhang H, *et al.* Microglial aryl hydrocarbon receptor enhances phagocytic function via SYK and promotes remyelination in the cuprizone mouse model of demyelination. *Journal of Neuroinflammation*. 2023; 20: 83. <https://doi.org/10.1186/s12974-023-02764-3>.
- [42] Cannon AS, Nagarkatti PS, Nagarkatti M. Targeting AhR as a Novel Therapeutic Modality against Inflammatory Diseases. *International Journal of Molecular Sciences*. 2021; 23: 288. <https://doi.org/10.3390/ijms23010288>.
- [43] Shackleford G, Sampathkumar NK, Hichor M, Weill L, Meffre D, Juricek L, *et al.* Involvement of Aryl hydrocarbon receptor in myelination and in human nerve sheath tumorigenesis. *Proceedings of the National Academy of Sciences of the United States of America*. 2018; 115: E1319–E1328. <https://doi.org/10.1073/pnas.1715999115>.
- [44] Haidar R, Shabo R, Moeser M, Luch A, Kugler J. The nuclear entry of the aryl hydrocarbon receptor (AHR) relies on the first nuclear localization signal and can be negatively regulated through IMP α/β specific inhibitors. *Scientific Reports*. 2023; 13: 19668. <https://doi.org/10.1038/s41598-023-47066-z>.
- [45] Zhou Y, Zhang J. Neuronal activity and remyelination: new insights into the molecular mechanisms and therapeutic advancements. *Frontiers in Cell and Developmental Biology*. 2023; 11: 1221890. <https://doi.org/10.3389/fcell.2023.1221890>.